Evolution of foam structures in Langmuir monolayers of pentadecanoic acid

Keith J. Stine, Steven A. Rauseo,* Brian G. Moore,
Joseph A. Wise, and Charles M. Knobler
Department of Chemistry and Biochemistry, University of California, Los Angeles, California 90024
(Received 4 January 1990)

Measurements are reported of the evolution of foam structures in monolayers of pentadecanoic acid at the air-water interface. The foams are observed by fluorescence microscopy. Various statistical properties of this random two-dimensional cellular structure have been determined: the second moment of the cell-side distribution is constant with time, the characteristic size grows according to a power law with an exponent ≈ 0.4, Aboav's law is obeyed, and the average cell perimeter is proportional to the number of sides. Comparisons are made with experiments on soap foams, metal grains, and simulations.

I. INTRODUCTION

Two-dimensional random cellular structures are ubiquitous in nature. They can be seen, for example, in the pattern of grain boundaries in thin metal or ceramic films[1] or in cross sections of bulk metals or ceramics;[2] soap foams trapped between parallel plates also have this form.[3-5] The apparent similarities in the structures for systems that have markedly different interactions suggests that there may be an underlying universal behavior, and this possibility has stimulated theoretical interest in the character and growth of such cellular patterns.

Atkinson[6] has recently discussed experiments, theories, and simulations relating to two-dimensional network structures; the thesis by Glazier[7] also contains a comprehensive review. We therefore provide only a brief overview of previous work.

Rivier[8] has used the principle of maximum entropy to derive structural equations of state for random space-filling cellular structures, a procedure which involves applying equilibrium statistical mechanical methods to nonequilibrium structures. A mean-field theory for the evolution of networks has been described by Fradkov *et al.*[9] and by Beenakker.[10] More detailed predictions about the structure are provided by the boundary migration model of Frost *et al.*[11] and the vertex motion models considered by Kawasaki and coworkers.[12]

A number of simulations of the growth of two-dimensional cellular structures have been performed. Weaire and Kermode[13] used a model in which an initial configuration of cells is allowed to relax toward an equilibrium configuration subject to the conditions that the vertices of a cell be trigonal and that the radius of curvature of each cell side is inversely proportional to the difference in pressure between adjoining cells. The area of a cell with n sides is then allowed to evolve with time in accord with von Neumann's law[14]

$$\frac{dA_n}{dt}=\kappa(n-6)\ . \tag{1}$$

Here κ is a constant that depends on the surface tension. von Neumann derived the law for the specific case of a two-dimensional network with trigonal vertices in which the structure evolves by diffusion of gas through the cell walls. It is assumed that the growth is driven by pressure differences proportional to the radii of curvature of the walls. Rivier[15] showed that the same relation can be obtained by purely topological arguments and therefore is more general.

Beenakker[16] has simulated foam growth with a continuum model, also based on Eq. (1), in which the coarsening of the network is described only in terms of A and n. The kinetics of domain growth in two dimensions after a temperature quench have been studied[17] by the Monte Carlo method applied to a Q-state Potts model; the boundaries between regions of different spin constitute a cellular structure.

The results of these theories and simulations can be represented in terms of several statistical measures of the cellular structure. One of these is $p(n)$, the probability of occurrence of a cell with n sides. For an infinite space-filling two-dimensional network with trigonal vertices, the Euler relation gives $\langle n\rangle=6$ for the first moment of this cell-side distribution. A correlation between the number of sides of a cell and m, the average number of sides of its neighbors, was found empirically by Aboav:[1]

$$mn=5n+8\ . \tag{2}$$

Weaire[18] suggested that Eq. (2) could be written as

$$mn=(6-a)n+(6a+\mu_2)\ , \tag{3}$$

where μ_2 is the second moment of the cell-side distribution and a is a constant of order unity. This expression was later derived by Lambert and Weaire;[19] Stavans and Glazier[4] showed that it holds very well for a soap foam.

Lewis,[20] from studies of biological systems, proposed that the average area of a cell, $\langle A_n\rangle$, should be a linear function of the number of sides, a relation now known as Lewis's Law. The law holds for mathematical mosaics generated by the Voronoi construction.[6] But for soap foams[5] and grain boundaries,[17,21] it is the average perimeter of the cells, $\langle P_n\rangle$, and not the area that is linear in n.

Rivier[8] has shown that the maximum entropy approach leads to the perimeter law when energy is carried by the interfaces between the cells.

It has been conjectured that the cell-side distribution approaches some stationary function with increasing time. Early experiments[3] and simulations[13] were ambiguous on this point, but recent measurements of soap foams,[4,22] and Potts model simulations[22] show that the second moment of the distribution becomes independent of time. The characteristic length scale of the network (e.g., average maximum linear dimension of a cell) is found to evolve with time according to a power law. Simulations of foams invariably give an exponent of $\frac{1}{2}$. Monte Carlo studies[17] of grain growth gave lower values, but more recent work[22,23] demonstrates that if the simulations are carried out to longer times an exponent of $\frac{1}{2}$ is also obtained. Power-law growth is observed in experiments, with exponents that vary from $\frac{1}{2}$ to about 0.35; a tabulation has been given by Glazier.[7] Note that he lists exponents for the area which are twice the values that we report.

Monolayer foams. Monolayers of amphiphilic molecules spread at the air-water interface can exhibit coexistence between a 2D gaseous phase (G) of low surface density and a denser liquidlike liquid-expanded (LE) phase.[24] A second coexistence region between the LE phase and a phase called the liquid-condensed (LC) phase exists at higher monolayer densities. The classical method of studying monolayer phase diagrams is by measuring isotherms of the surface pressure Π as a function of surface density. For a one-component monolayer (at constant external pressure p), the phase rule requires that Π be constant when there is coexistence between two phases (see Fig. 1).

If a small amount ($\approx 0.5-1.5$ mol %) of a fluorescent probe is added to the monolayer, coexisting LE and G (or LE and LC) domains can be distinguished with the technique of fluorescence microscopy.[25] The contrast between the phases results from differences in surface density or differences in solubility of the probe between the two phases. It is also known that the fluorescence of some probes is quenched in the gas phase.[26]

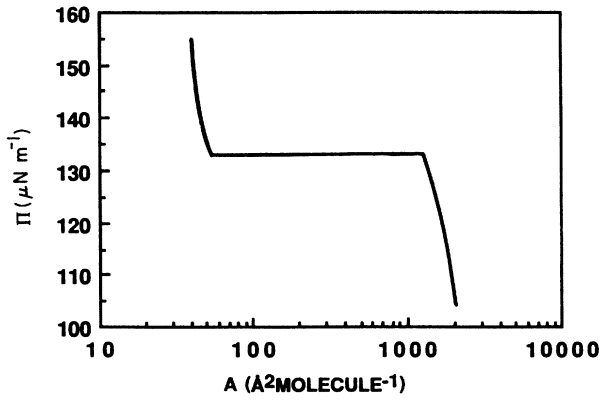

FIG. 1. Surface pressure-area isotherm for pentadecanoic acid at 20°C. The LE-LC transition region occurs at much higher pressures and smaller area.

Moore *et al.*[26] used the fluorescence technique to investigate stearic acid monolayers and discovered the existence of random cellular structures when the monolayer was deposited at densities at which the LE and G phases coexist. Such foamlike structures have now been observed by fluorescence microscopy in the LE-G coexistence regions of monolayers of other fatty acids[27] and of several methyl and ethyl esters.[28,29]

Although the investigations on stearic acid monolayers were not extensive, Moore *et al.*[26] were able to determine a rough cell-side distribution and to show that the characteristic size of the foam appeared to grow according to a power law. It was clear from these results that the monolayer foam was similar to other random two-dimensional cellular structures. In this paper we report a quantitative study of monolayer foams. The measurements have been carried out on monolayers of pentadecanoic acid (PDA), a system for which extensive fluorescence studies and isotherm measurements have been performed[27,30]

II. EXPERIMENT

Pentadecanoic acid from Nu-Chek Prep, Inc. (stated purity >99%) was used without further purification. The fluorescent probe, NBD-HDA [4-(hexadecylamino)-7-nitrobenz-2-oxa-1,3-diazole], was obtained from Molecular Probes, Inc. A solution of PDA in Fisher reagent grade chloroform was prepared and a measured amount of a stock solution of NBD-HDA in chloroform was added by pipet. The concentration of the PDA+probe solution used was 2.74×10^{14} molecules/$\mu\ell$ and contained 1.2 mol % probe.

The Langmuir trough and fluorescence microscope used have been described previously.[27,28] The upper part of the trough containing the acidified subphase and monolayer is made of Teflon. This portion is separated by a 0.8-mm-thick Teflon sheet from thermostated water circulating in the hollow aluminum base, which rests on the translation stage of the microscope. The dimensions of the water surface are 8.0×2.5 cm^2. All of the foam observations reported here were made at 20°C. A 0.15-mm-thick glass coverslip was used to cover the trough.

The monolayer was formed by depositing the solution of the amphiphile on the water surface using a Hamilton syringe and allowing the chloroform to evaporate. The water used was purified in a Milli-Q system with an organics filter and was then acidified to pH 2 using HCl which was doubly distilled from the azeotrope.

Images were obtained with a Reichert-Jung Polyvar Met microscope with epifluorescence attachment. Light from a mercury lamp is focused on the monolayer through the objective and excites the probe fluorescence. The fluorescence image is separated from the exciting light with a dichroic mirror and is observed with a SIT television camera and recorded. Magnifications of 16× and 8× were employed and the resolution was about 3 μm

Images of the foam structure on a 24-in. monitor were digitized with a model GP-7 Grafbar Mark II sonic digi-

tizer (Science Accessories Corporation) interfaced to an IBM personal computer. An image was frozen on the monitor and the coordinates of the vertices of each foam cell were registered using the digitizer pen. The positions of the vertices of a cell, which could be located with a precision of 1 mm, were recorded by proceeding sequentially around the perimeter back to the first digitized vertex. (The size of the images on the monitor correspond to an effective magnification of 300 when the 16× objective is used.) The sets of vertex coordinates, one for each cell, were saved in a data file for processing by a statistics program.

Foam preparation. An isotherm of PDA at 20 °C is shown schematically in Fig. 1. The molecular area of the LE phase that coexists with the gas is 45 Å^2/molecule as determined independently by the isotherm measurements of Pallas and Pethica[31] and the fluorescence microscopy observations of Moore *et al.*;[27] that of the gas phase is 1500 Å^2/molecule as determined from the isotherm data. One might expect that the formation and growth of the foam structure would most easily be generated by a rapid expansion from the LE phase or a temperature quench into the coexistence region from the one-phase region. We found, however, that when the foam was produced by rapid expansion from the LE phase to roughly 300 Å^2/molecule by rapidly moving a Teflon barrier, flows were generated in the monolayer that take about 2 min to subside, and the resulting foam is very nonuniform. The temperature quench approach was not possible because the LE-G coexistence in PDA persists to temperatures well in excess of 40 °C at densities at which a large connected foam structure might be expected to form.[27,31] Monolayer studies at such elevated temperatures are very difficult to accomplish.

For a PDA film spread at 20 °C to 61 Å^2/molecule, a lever-rule calculation gives an area fraction for the LE phase of 0.73. We have found that foam growth can be consistently observed at roughly 55–80 Å^2/molecule by the addition of solvent. After spreading, a portion of the monolayer is left uncovered by shifting the position of the coverslip. One then observes that this side of the trough becomes completely covered by the LE phase, while foam cells are found in the covered section. Experiments in which the position of the coverslip was varied and at different monolayer temperatures relative to the room temperature show that this effect is not caused by temperature gradients or flows. It is likely the result of the change in the humidity of the air above the film, which produces small changes in the surface tension. While such changes are usually negligible,[32] they can be significant at the low surface pressures at the LE-G transition, which are of the order of 100 μN m^{-1} for PDA at room temperature.[31] If the surface density is decreased the monolayer tends to consist of islands with a small number of cells and droplets of the LE phase.

On addition of 0.5 $\mu\ell$ of chloroform with a syringe, the surface pressure jumps to $\approx$0.5 mN m^{-1} and drives all of the monolayer out of the two-phase region and into the LE phase. The chloroform evaporates and Π relaxes back to the equilibrium value of $\approx$100 μN m^{-1} in 60–90 sec. As the solvent evaporates and the monolayer reenters the two-phase region, the gas phase nucleates randomly in the covered side of the trough. The 2D bubbles grow and evolve to a foam structure with small cells within 50–70 sec. The foam then begins to evolve and grow. We have also used hexane to compress the monolayer and found the same behavior as with chloroform.

In our experiments, the foam growth was followed for about 30 min with the magnification switched from 16×

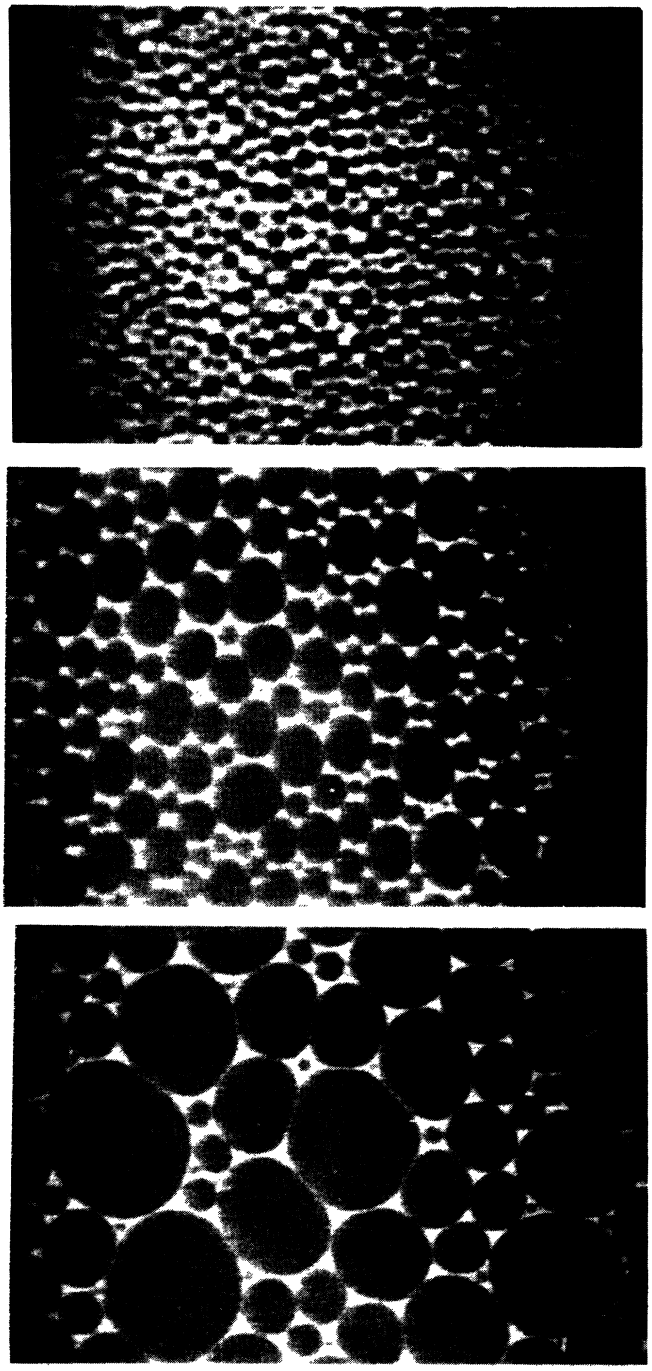

FIG. 2. Evolution of a PDA monolayer foam. The experiment (run 1) was carried out at 20 °C and at an area of 61 Å^2 molecule^{-1}. Times after addition of chloroform: (a) 66 sec; (b) 98 sec; (c) 397 sec. The bar in (b) represents 100 μm

to 8× after about 300 sec to allow observation of more cells. A series of images of the evolution of the monolayer foam structure is shown in Fig. 2. The foam statistics were obtained by averaging two–four images within logarithmically spaced time bins for two of the runs. Since the digitizing process is very time consuming, the images from the other two runs were used only to obtain the time dependence of the average cell size by counting the number of cells in a fixed area on the screen. The number of cells in a time bin typically varied from 200 for the first bin to 100 for the last.

III. RESULTS

The monolayer foam structure evolves almost exclusively by two elementary processes:[33] the switching of neighboring vertices (T1) and the disappearance of three-sided cells (T2). We have counted the number of processes of each type in a typical run. At the start, the rate of T1 processes is roughly 8×10^{-3} cell^{-1} sec^{-1} and by 200 sec it has fallen by a factor of 8. The rate of T2 processes is about $\frac{1}{3}$ that of the T1 rate. Inverse mitosis, which occurred in stearic acid foams,[26] was observed only once (in run 3). We often observe that three-sided cells shrink to a vertex that contains a small circular bubble. (We have treated such cell remnants as vertices in compiling the foam statistics.) The foam structure begins to break down after about 4 h and changes into islands of liquid containing round gas bubbles.

The cell-side distributions $p(n)$ were obtained for the two digitized runs. Figure 3 is a plot of μ_2 as a function of time. The two runs are indistinguishable; μ_2 is best described as being constant and has the value $\mu_2=2.01\pm0.66$ for run 3 and $\mu_2=1.89\pm0.68$ for run 4. The constancy of μ_2 suggests a time-independent distribution, and histograms of the time-averaged cell-side distributions are presented in Fig. 4. It is evident that within the experimental uncertainties, the two distributions are indistinguishable; the combined distributions give $\langle n\rangle=5.88\pm0.08$. Values of $\langle n\rangle$ below 6 are to be expected[2] for samples of finite size because large cells are more likely to intersect field boundaries than small cells and are therefore excluded from the count of complete cells.

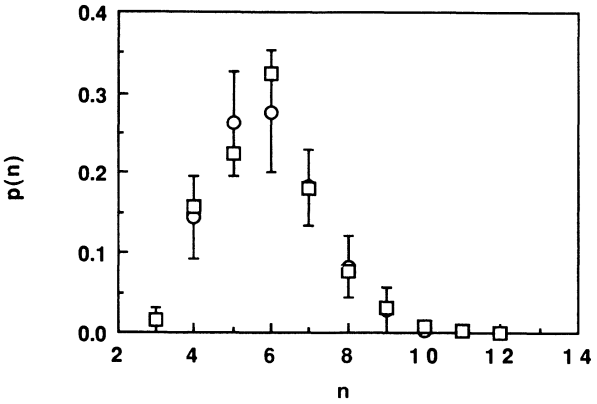

FIG. 4. Cell-side distributions for runs 3 and 4. Symbols as in Fig. 3. For clarity, error bars are shown only for run 3; those for run 4 are similar.

The product of the number of sides of a cell and m, the average number of sides of its neighbors, is linear in n at all times; the time average of mn plotted against n is shown in Fig. 5. A linear least-squares fit to these data for $n=3-10$ yields 4.74 ± 0.04 as the slope and 8.62 ± 0.30 as the intercept. If we interpret these as in Eq. (2), we obtain $a=1.26\pm0.04$ and $\mu_2=1.06\pm0.54$. It is possible to test for consistency between the measured value of μ_2 and that calculated from the slope and intercept of the fit to the Aboav relation. The value of μ_2 obtained this way agrees (within the overlap of the large uncertainties) with that found from the analysis of the cell-side distributions.

Figures 6(a) and 6(b) show, respectively, the average area and perimeter plotted against n. The perimeter law provides a good representation of the data: a weighted linear least-squares fit gives $\chi_\nu^2=0.70$. Lewis's law fails. The fit for the area gives $\chi_\nu^2=20$ and leads to negative values for the areas of cells with fewer than four sides.

We have examined the growth rate of the average cell diameter D by fitting the data to the expression

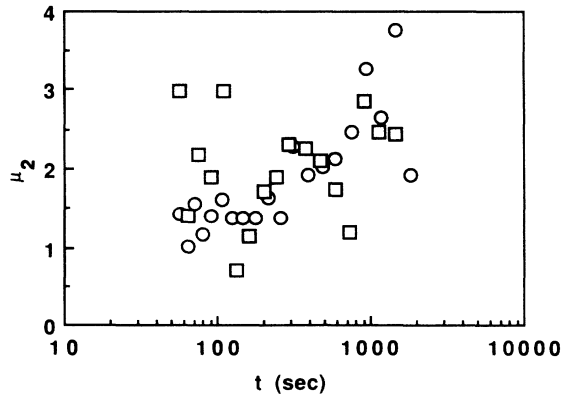

FIG. 3. Second moment μ_2 as a function of time. Run 3, circles; run 4, squares.

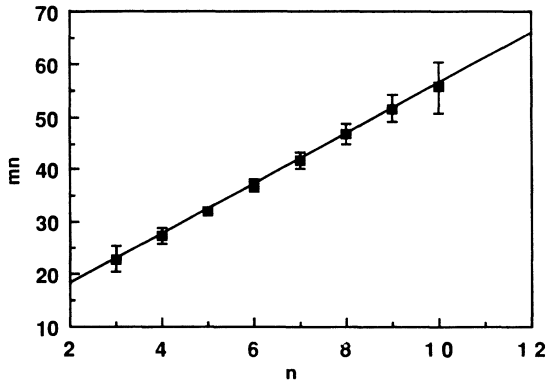

FIG. 5. Test of Aboav's law.

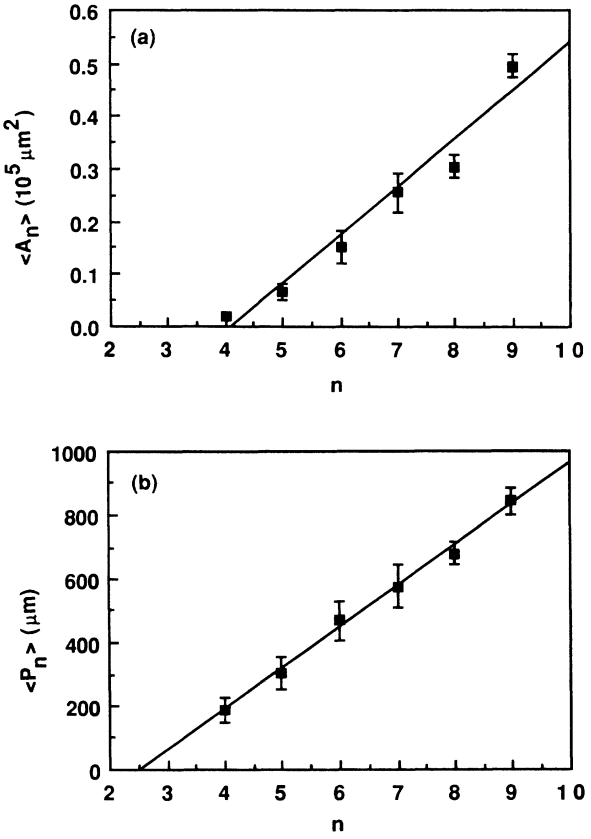

FIG. 6. (a) Average cell area $\langle A_n \rangle$ as a function of n; (b) average cell perimeter $\langle P_n \rangle$ as a function of n. The lines represent weighted linear least-squares fits to the data.

$$D = D_0 + B(t - t_0)^{\alpha} , \tag{4}$$

where t_0 is the time at which the foam structure was first observed after the addition of the chloroform and D_0 is the average diameter at that time. For simplicity, the diameters were calculated from the cell areas: $D = (4A)^{1/2}/\pi$; averages of other measures of the characteristic size, such as the maximum distance between vertices or the ratio of the area to the perimeter, are found to differ only by constant factors from D. Values of t_0 and D_0 could be bracketed by observation. The time at

TABLE I. Values of growth exponent α, amplitude B, and their standard errors obtained from linear least-squares fits for different choices of t_0 and D_0.

Data set	t_0 (sec)	D_0 (μm)	B (μm)	α
1	66.0	22.0	6.9±1.1	0.36±0.01
1	71.0	27.5	5.0±1.1	0.40±0.01
2	63.0	20.4	5.5±1.1	0.39±0.01
2	66.0	25.5	3.1±1.2	0.46±0.03
3	32.0	24.5	25.3±1.2	0.25±0.04
3	36.0	27.8	23.9±1.2	0.25±0.04
4	44.0	27.2	8.3±1.2	0.36±0.03
4	49.0	32.4	6.7±1.2	0.38±0.04

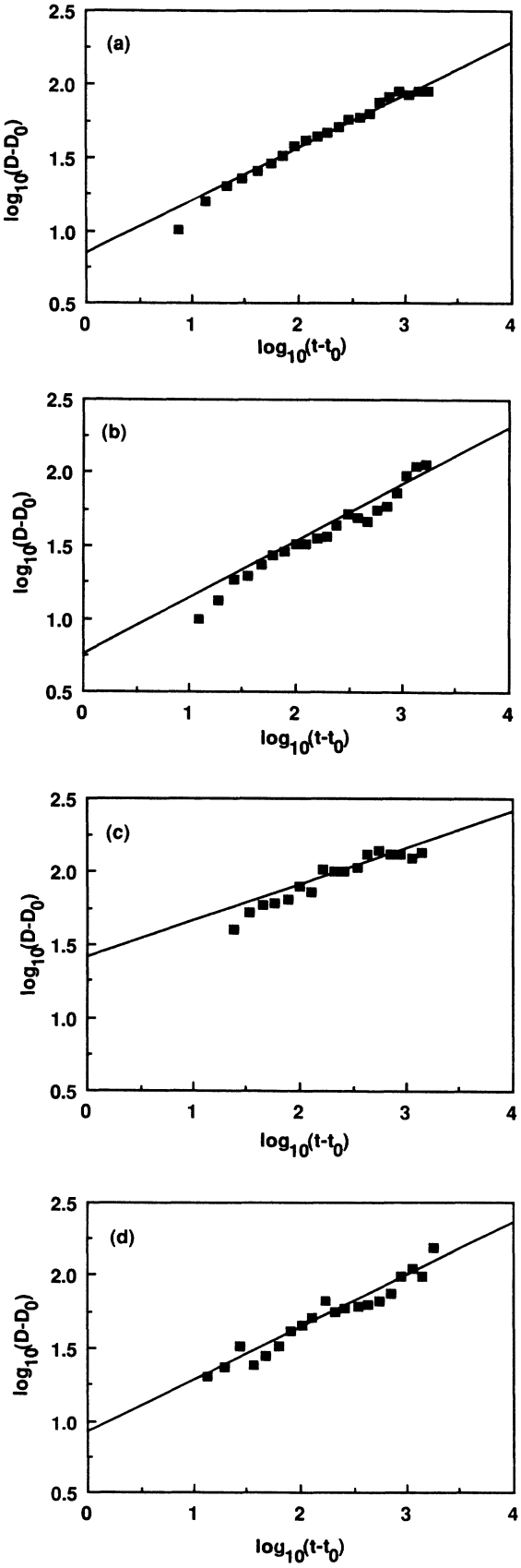

FIG. 7. $\log_{10}(D - D_0)$ as a function of $\log_{10}(t - t_0)$. The lines represent least-squares fits with the earlier values of t_0 and D_0 shown in Table I. (a) Run 1; (b) run 2; (c) run 3; (d) run 4.

which foam cells could first be distinguished from growing bubbles was taken as the lower limit of t_0 and that at which the image of the foam cells was first sharp and unambiguous was chosen as the upper limit. The limits of D_0 were taken as the measured values at the t_0 limits.

Linear least-squares fitting of $\log_{10}(D-D_0)$ versus $\log_{10}(t-t_0)$ was performed for $t>90$ sec after the addition of the chloroform. The two sets of t_0 and D_0 values are presented in Table I along with the corresponding growth exponents, growth amplitudes, and their standard errors. Figures 7(a)–7(d) show $\log_{10}(D-D_0)$ plotted against $\log_{10}(t-t_0)$ for the four runs and the least-squares lines for the earlier choices of t_0; the fits for the other choices of t_0 and D_0 are comparable in quality.

Runs 1, 2, and 4 give comparable values of the growth-law exponent and prefactor; run 3, despite the close similarity of its cell-side distribution to that of run 4, has a much lower exponent and a much larger prefactor. We have not been able to find a reason for these differences.[34] We believe that the smaller values of t_0 more accurately reflect the initial state of the foam. For this choice, the average value of α is 0.34 ± 0.05 including run 3 and 0.37 ± 0.06 without it. The later times give values about 0.04 larger.

We have made only a rough study of the growth rate of cells as a function of their area. von Neumann's law, Eq. (1), does not appear to hold. The rate at which cells with $n<6$ shrink is slower than that at which cells with $n>6$ grow and we therefore do not observe a growth rate proportional to $n-6$.

The distribution of cell areas at three times was determined for the digitized runs. Histograms of $p(A/\langle A\rangle)$, the fraction of cells within a given range of area, plotted against $A/\langle A\rangle$ are shown in Fig. 8 for run 3; the distributions for run 4 are similar. In general, $p(A/\langle A\rangle)$ decreases with increasing area although there also appears to be a peak in the distribution near $A/\langle A\rangle=1$. The largest cells that have been observed have areas $\approx 5\langle A\rangle$.

Stability requires that the angles at the vertices of a 2D soap foam should average to 120°. We have measured the distribution of angles as a function of n for three representative frames for $t-t_0=60$, 120, and 360 sec by sketching the pattern on the monitor and using a protractor to measure the angles; the result is shown in Fig. 9. The average of the 283 cell vertex angles examined was $120°\pm13°$. There is broad distribution of angles for each value of n. The average vertex angle increases from $\approx 105°$ for $n=4$ and levels off at $\approx 125°$ for $n\geq 7$.

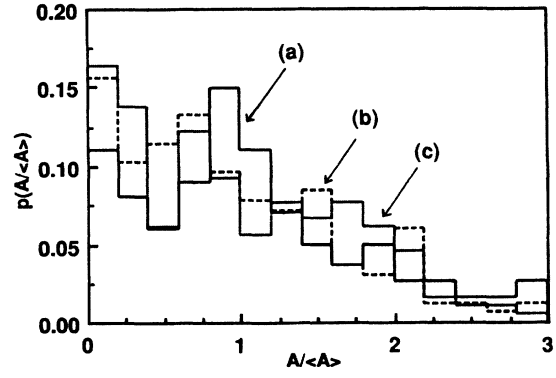

FIG. 8. Distribution of areas for run 4. Values of $t-t_0$: ——, 58–71 sec; — — —, 214–309 sec; · · · ·, 1165–1825 sec.

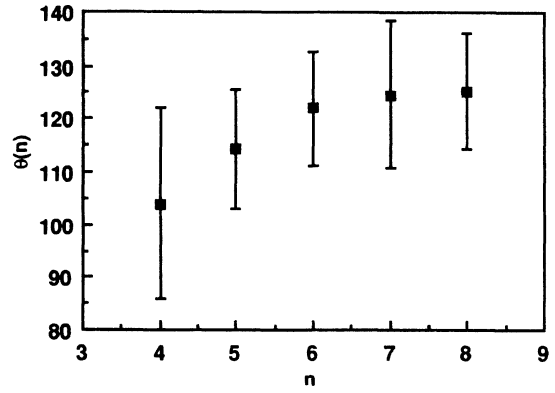

FIG. 9. Distribution of vertex angles as a function of n. The bars show the range of angles observed for each value of n.

IV. DISCUSSION

The monolayer foam side distribution is compared in Fig. 10 with distributions for foams and grain boundaries derived from simulations and experiments. For clarity, we have suppressed the error bars, which were shown in Fig. 3, but these should be remembered in drawing conclusions.

Kawasaki and co-workers have described[12,35] several two-dimensional vertex models, which differ in the degree of approximation. Their models I and II (Ref. 12) agree quite well with our distributions for larger cells, but like the soap foams, have five-sided cells as the most probable. This is also the case with the Potts model calculations,[17,22] which otherwise match the monolayer foam

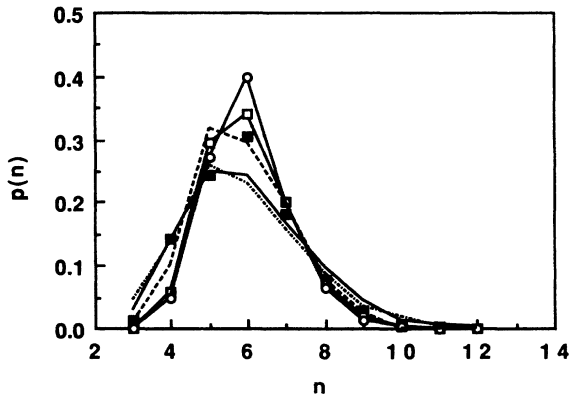

FIG. 10. Comparison of cell-side distributions. This work, ■; vertex model II, Kawaski *et al.* (Ref. 8), ——; vertex model 0, Kawasaki *et al.* (Ref. 26), □; continuum model, Beenakker (Ref. 11), ○; soap foams, Stavans and Glazier (Ref. 4), — — —; Potts model, Srolovitz *et al.* (Ref. 12), —·—·—·.

distribution very well.

In recent work, Kawasaki, *et al.*[35] have introduced a third model, model *O*, which allows for anisotropy. This model gives a distribution peaked at 6, but which is much narrower than those for either models I and II or our experimental one. The distribution in Beenakker's continuum model[16] also has its maximum at 6, but the probability of six-sided cells is much higher than we have observed and that of four-sided cells is much lower. His mean-field theory[10] predicts that the growth rate will alternate between slow and fast regimes with concurrent broadening and collapse of the cell side distribution, which becomes bimodal with $\mu_2 \approx 3$ before collapse. We observed two histograms for individual time bins where the percentage of five- and seven-sided cells is slightly greater than that of the six-sided cells, but we do not find an oscillation in μ_2 that can be matched to a trend in the histograms of the individual time bins.

The monolayer foam distribution can be compared with those determined from the recent soap foam experiments,[4,22] which have been summarized by Glazier.[7] For the soap foams, the maximum in the distribution occurs consistently at 5, rather than 6, although the differences are generally small and the variation between runs significant. For example, in the most recent measurements[22] the probabilities of five- and six-sided cells were 0.292 and 0.285, respectively, while the averages[7] for all measurements were 0.314 ± 0.023 and 0.305 ± 0.017. Stavans and Glazier[4] reported a second moment of 1.4 ± 0.1; in more recent experiments,[22] μ_2 was found to be 2.5 ± 0.3. Our determinations of the second moment lie close to the average of these values.

The poor statistics in the distributions determined by Moore *et al.*[26] in stearic acid monolayers made it difficult to determine the values of the second moment. It was noted, however, that μ_2 appeared to increase with time. We have made a preliminary reinvestigation of stearic acid using the methods employed for PDA.[36] In contrast to the earlier work, we do not see any increase in time; the stearic acid data can be represented by a constant value $\mu_2 = 2.80 \pm 0.81$, which is larger than that found for PDA. This is consistent with the observation that stearic acid foams contain more large many-sided cells (up to $n = 15$) than are found in PDA. The difference may be attributable to the larger line tension between the phases in stearic acid.

Time invariance of μ_2 has been observed in a number of simulations. Srolovitz *et al.*[17] found $\mu_2 \approx 2.2$ in their Potts model simulations of grain growth; $\mu_2 = 2.4 \pm 0.1$ was obtained when the simulation was extended to longer times.[22] In another Monte Carlo study, Wejchert, Weaire, and Kermode[37] found $\mu_2 = 1.8 \pm 0.05$ for the steady-state value in a model appropriate to grain growth and 1.6 ± 0.1 for one simulating the growth of a soap froth.

Our determination of the growth exponent α is not very precise, but the value $\alpha = 1/2$, which can be obtained[5,13(b)] by dimensional arguments for a system that follows von Neumann's law and that is found in many simulations of foams,[12,16,35,37] can be excluded. The experiment of Glazier *et al.*[5] on a soap foam gave $\alpha = 0.30 \pm 0.05$, which is compatible with the average of the values we observed. Glazier and Stavans[38] suggest that their failure to observe $\alpha = \frac{1}{2}$ in the soap-foam experiments may have been the result of fluid drainage from the Plateau borders onto the lower glass plate. As the film on the plates thickens, the height of the cells, and thus the effective area for diffusion between them, decreases, which should reduce the overall growth rate. They note that experiments in which the plate spacing was $\frac{1}{8}$ in gave $\alpha = 0.35$ while those with a $\frac{1}{16}$-in. spacing gave a value of 0.29. Glazier[7] states that experiments in $\frac{1}{8}$-in cells give results "consistent with, though not conclusively demonstrating" $\alpha = \frac{1}{2}$.

The drainage mechanism cannot exist in the monolayer foams. It is conceivable that the low values of α arise because the foam is not well developed in the initial stages of our experiments and we are observing the growth of individual droplets.[34] We have been unable to extend our measurements to longer times to see if there is any tendency for the growth to speed up, so we are unable to test this hypothesis.

Rivier and Lissowski[39,8] have argued that the failure of Lewis's law is evidence for the existence of constraints on the cellular structure other than those imposed by topology and the requirement of filling space. Experiments on grain boundaries[40] show that the perimeter (or diameter) is linear in n, a result found as well in simulations of grain boundary growth.[17] Weaire and Kermode[13(b)] determined from their simulation of a soap froth that plots of $\langle A_n \rangle$ against n curved up at lower n, a tendency also found in the soap-foam measurements by Glazier *et al.*[5]

The area distribution more closely resembles an exponential than the roughly log-normal distributions found in the vertex-model simulations.[12] The similarity to the distributions found in the Potts model simulations[17,23] and experiments on grain growth[21] is more apparent when the area distribution histogram is converted[8] into a plot of $p(A/\langle A \rangle)$ against $\log_{10}(A/\langle A \rangle)$ (Fig. 11). Rivier's maximum entropy approach leads to an exponential distribution of cell areas when the energy is constrained.[8]

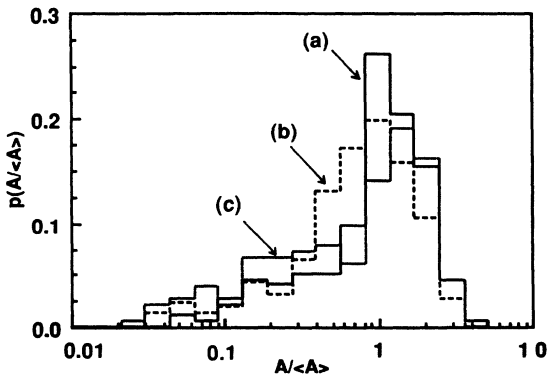

FIG. 11. Area distribution as a function of $\log(A/\langle A \rangle)$ for run 4. The meaning of the line types is the same as in Fig. 8.

The distribution of angles in the monolayer foam is quite similar to that observed by Stavans and Glazier,[4] who generalized the von Neumann law to vertex angles other than 120°. For the distribution of angles that we observe, the modified law leads to an increase in the magnitudes of both the rates of appearance and disappearance of cells, and therefore cannot account for our observation that cells with $n < 6$ seem to shrink more slowly than predicted by von Neumann's law. Strain induced by the deviations from 120° favors T1 processes,[33] which may account for the relatively high fraction of cells with small areas that we observe. The 3:1 ratio of T1 to T2 processes in the monolayer foams is markedly different from the 1:1 ratio found in vertex models I and II (Ref. 12) or the complete neglect of T1 processes in the Beenakker simulation.[16] It is not clear how these differences affect the structures of the networks.

Although the networks in the monolayers appear very similar to those in the soap foams, one should recognize that there are some fundamental differences between the systems. Molecules of PDA are dipolar and in condensed phases they are to some extent aligned perpendicular to the water surface.[24,41] The textures that are observed in monolayers are thought to arise from a balance between the repulsive dipole-dipole interaction, which favors extended structures, and the line tension, which tends to minimize boundaries.[42] Andelman *et al.*[43] predict that this balance can lead to the existence of stable, density modulated phases at molecular areas typical of G-LE equilibrium.

If the long-range dipolar forces impose an optimum wavelength on the monolayer, then the foam side distribution will be affected: the frequencies of cells with sizes smaller and larger than the optimum wavelength will be smaller than those expected for a foam in statistical equilibrium. Glazer[7] has argued that such wavelength selection occurs in magnetic bubble patterns, in which the side distribution is very narrow and peaks at 6, rather than 5.

We have observed[29] labyrinth structures similar to those seen in magnetic bubbles in monolayers of fatty acids, but only as a transient phenomenon after large temperature quenches from a one-phase region. Can the maximum in the side distribution at $n = 6$ be attributed to existence of an optimum wavelength in the pattern? This seems unlikely. As seen in Fig. 10, while the number of five-sided cells in the monolayer network is small with respect to that found in the soap foams, the numbers of smaller cells in the monolayer differ little from those found in the soap foam. There is also no evidence of suppression of many-sided cells. Given the rather larger uncertainties in the distributions, a more detailed analysis of the differences between the soap and monolayer foams does not appear fruitful.

Note added in proof. Stavans[44] has observed vertex angles of 120° and a growth exponent $\alpha = \frac{1}{2}$ in drained soap foams.

ACKNOWLEDGMENTS

This work was supported by the National Science Foundation. One of us (J.W.) acknowledges the support of the Research Corporation. We thank F. Rondelez for helpful discussions and the referee for many useful suggestions.

*Present address: Naval Surface Warfare Center, Silver Spring, MD 20903-5000.

[1]D. A. Aboav, Metallogr. **3**, 383 (1970).

[2]M. Blanc and A. Mocellin, Acta. Metall. **27**, 1231 (1979).

[3]C. S. Smith, in *Metal Interfaces,* edited by C. Herring (American Society for Metals, Cleveland, OH, 1952), pp. 65–108.

[4]J. Stavans and J. A. Glazier, Phys. Rev. Lett. **62**, 1318 (1989).

[5]J. A. Glazier, S. P. Gross, and J. Stavans, Phys. Rev. A **36**, 306 (1987).

[6]H. V. Atkinson, Acta Metall. **36**, 469 (1988).

[7]J. A. Glazier, Ph.D. dissertation, Department of Physics, University of Chicago, 1989.

[8]N. Rivier, Philos. Mag. B **52**, 795 (1985).

[9]V. E. Fradkov, L. S. Shvindlerman, and D. G. Udler, Scripta Met. **19**, 1285 (1985).

[10]C. W. J. Beenakker, Phys. Rev. Lett. **57**, 2454 (1986).

[11]H. J. Frost, C. V. Thompson, C. L. Howe, and J. Whang, Scripta Met. **22**, 65 (1988).

[12]K. Kawasaki, T. Nagai, and K. Nakashima, Philos. Mag. B **60**, 399 (1989).

[13](a) D. Weaire and J. P. Kermode, Philos. Mag. B **48**, 245 (1983); (b) **50**, 379 (1984).

[14]J. von Neumann, Ref. 3, p. 108.

[15]N. Rivier, Philos. Mag. B **47**, L45 (1983).

[16]C. W. J. Beenakker, Phys. Rev. A **37**, 1697 (1988).

[17]D. J. Srolovitz, M. P. Anderson, P. S. Sahni, and G. S. Grest, Acta Metall. **32**, 793 (1984); Phys. Rev. Lett. **50**, 263 (1983).

[18]D. L. Weaire, Metallogr. **7**, 157 (1974).

[19]C. J. Lambert and D. L. Weaire, Metallogr. **14**, 307 (1981).

[20]F. T. Lewis, Anat. Rec. **38**, 341 (1928).

[21]D. A. Aboav and T. G. Langdon, Metallogr. **2**, 171 (1969).

[22]J. A. Glazier, M. P. Anderson, and G. S. Grest, Philos. Mag. B (to be published).

[23]G. S. Grest, M. P. Anderson, and D. J. Srolovita, in *NATO Advanced Study Institute on Time-Dependent Effects in Disordered Materials,* edited by R. Pynn and T. Riste (Plenum, New York, 1987), p. 365.

[24]G. L. Gaines, Jr., *Insoluble Monolayers at Liquid-Gas Interfaces* (Wiley, New York, 1966).

[25]V. von Tscharner and H. M. McConnell, Biophys. J. **36**, 409 (1981); M. Lösche, E. Sackmann, and H. Möhwald, Ber. Bunsenges. Phys. Chem. **87**, 848 (1983).

[26]B. Moore, C. M. Knobler, D. Broseta, and F. Rondelez, J. Chem. Soc. Faraday Trans. II **82**, 1753 (1986) (see also addenda on pp. 1851, 1852).

[27]B. G. Moore, C. M. Knobler, S. Akamatsu, and F. Rondelez, J. Phys. Chem. **94**, 4588 (1990).

[28]B. G. Moore, Ph.D. dissertation, Department of Chemistry, University of California, Los Angeles, 1989.

[29]K. Stine, B. G. Moore and C. M. Knobler, unpublished.

[30]After this paper was submitted, we learned about investigations of PDA foams by B. Berge, A. J. Simon, and A. Libchaber; following paper, Phys. Rev. A **41**, 6893 (1990).

[31]N. R. Pallas and B. A. Pethica, J. Chem. Soc. Faraday Trans.

I **83**, 585 (1987).

[32]N. R. Pallas and B. A. Pethica, Colloids and Surfaces **6**, 221 (1983).

[33]D. Weaire and N. Rivier, Contemp. Phys. **25**, 59 (1984).

[34]The disparate behavior of run 3 might indicate that a network structure had not developed at early times and, as a result, we were observing the growth of individual droplets, whose diameters would be expected to grow as $t^{1/3}$ [Lifschitz-Slyozov mechanism (Ref. 6)] [J. Glazier (private communication)]. This might be the case, for example, if the gas-to-liquid ratio were lower in run 3 than in the other runs. We have estimated this ratio by analyzing (Ref. 27) the relative white and black areas in the images, and found no significant differences between the runs. Crossover might also be implicated if there were a clear change in the polygonality of the cells during a run. This is difficult to determine objectively, but again, after reviewing the tapes, we see no apparent differences between the runs. Since we observe only small sections of the foam at any one time during the measurements, it is possible that the difference between the runs is a result of heterogeneity. The problem is likely to be resolved only by further measurements, which we intend to carry out.

[35]K. Kawasaki, T. Nagai, and S. Ohta (unpublished).

[36]K. Stine, J. Wise, and C. Knobler (unpublished).

[37]J. Wejchert, D. Weaire, and J. P. Kermode, Philos. Mag. B **53**, 15 (1986).

[38]J. A. Glazier and J. Stavans, Phys. Rev. A **40**, 7398 (1989).

[39]N. Rivier and A. Lissowski, J. Phys. A **15**, L143 (1982).

[40]See, e.g., D. A. Aboav and T. G. Langdon, Meteallogr. **2**, 171 (1969).

[41]C. M. Knobler, in *Advances in Chemical Physics,* edited by I. Prigogine and S. Rice (Wiley, New York, 1990), Vol. 77, p. 397.

[42]See, for example, H. M. McConnell and V. T. Moy, J. Phys. Chem. **92**, 4520 (1988).

[43]D. Andelman, F. Brochard, and J. F. Joanny, J. Chem. Phys. **86**, 3673 (1987).

[44]J. Stavans (private communication).

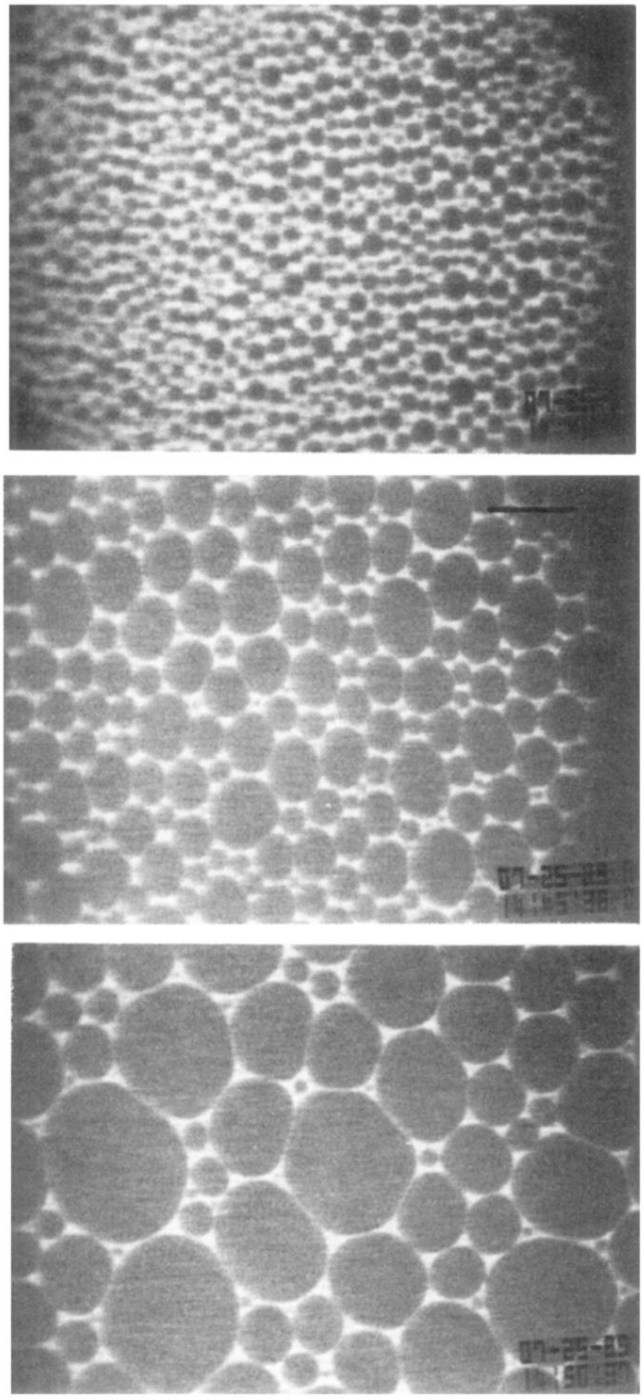

FIG. 2. Evolution of a PDA monolayer foam. The experiment (run 1) was carried out at 20 °C and at an area of 61 $Å^2$ molecule^{-1}. Times after addition of chloroform: (a) 66 sec; (b) 98 sec; (c) 397 sec. The bar in (b) represents 100 μm